RNA four-way junction (4WJ) for spontaneous cancer-targeting, effective tumor-regression, metastasis suppression, fast renal excretion and undetectable toxicity

Xin Li [a,b,1], Kai Jin [a,b,1], Tzu-Chun Cheng [e], You-Cheng Liao [f], Wen-Jui Lee [a,b], Abhjeet S. Bhullar [a,b], Li-Ching Chen [g], Piotr Rychahou [h], Mitch A. Phelps [a,b], Yuan Soon Ho [e,**], Peixuan Guo [a,b,c,d,*]

[a] Division of Pharmaceutics and Pharmacology, College of Pharmacy, The Ohio State University, Columbus, OH, 43210, USA
[b] Center for RNA Nanotechnology and Nanomedicine, The Ohio State University, Columbus, OH, 43210, USA
[c] James Comprehensive Cancer Center, College of Medicine, The Ohio State University, Columbus, OH, 43210, USA
[d] Dorothy M. Davis Heart and Lung Research Institute, College of Medicine, The Ohio State University, Columbus, OH, 43210, USA
[e] Institute of Biochemistry and Molecular Biology, China Medical University, Taichung, 406040, Taiwan
[f] Graduate Institute of Medical Sciences, College of Medicine, Taipei Medical University, Taipei, 110031, Taiwan
[g] Department of Biological Science & Technology, China Medical University, Taichung, 406040, Taiwan
[h] Markey Cancer Center, Department of Surgery, University of Kentucky, Lexington, KY, 40536, USA

ARTICLE INFO

ABSTRACT

The field of RNA therapeutics has been emerging as the third milestone in pharmaceutical drug development. RNA nanoparticles have displayed motile and deformable properties to allow for high tumor accumulation with undetectable healthy organ accumulation. Therefore, RNA nanoparticles have the potential to serve as potent drug delivery vehicles with strong anti-cancer responses. Herein, we report the physicochemical basis for the rational design of a branched RNA four-way junction (4WJ) nanoparticle that results in advantageous high-thermostability and -drug payload for cancer therapy, including metastatic tumors in the lung. The 4WJ nanostructure displayed versatility through functionalization with an anti-cancer chemical drug, SN38, for the treatment of two different cancer models including colorectal cancer xenograft and orthotopic lung metastases of colon cancer. The resulting 4WJ RNA drug complex spontaneously targeted cancers effectively for cancer inhibition with and without ligands. The 4WJ displayed fast renal excretion, rapid body clearance, and little organ accumulation with undetectable toxicity and immunogenicity. The safety parameters were documented by organ histology, blood biochemistry, and pathological analysis. The highly efficient cancer inhibition, undetectable drug toxicity, and favorable Chemical, Manufacturing, and Control (CMC) production of RNA nanoparticles document a candidate with high potential for translation in cancer therapy.

1. Introduction

It was predicted that RNA therapeutics would be the third milestone in drug pharmaceutical drug development [1,2]. Now the spring of RNA therapeutics is coming. Nanoparticles have been developed as drug delivery platforms with the goal to improve the therapeutic outcome of small molecule drugs by increasing solubility and stability, improving bioavailability, extending circulation time, and reducing side effects [3–5]. Ribonucleic acid (RNA) is a novel biomaterial used to construct novel nanoparticles to deliver drugs for disease treatment. RNA nanoparticles with various two- and three-dimensional (2D and 3D) structures have been constructed using bottom-up assembly, rolling circle transcription, and RNA origami approaches [6–12]. RNA nanoparticles have many advantages, such as net negative charge for repulsion to nontargeted cells, multivalence for multiple conjugates, programmability, one-pot self-assembly from short oligos, and favorable

---

biodistribution profile, that make them suitable as drug delivery platforms [13–17].

RNA nanoparticles are highly programmable in terms of size, shape, stability, and stoichiometry [18–22]. Short RNA strands can be synthesized through solid-phase synthesis with various of modifications with defined quantity and position. Multi-functional RNA nanoparticles can be easily produced by mixing functionalization RNA strands at a defined molar ratio with high assembly efficiency [9,23]. This allows for the Chemical, Manufacturing, and Control (CMC) production of RNA nanoparticles, which makes them feasible for clinical applications. Furthermore, RNA nanoparticles have been functionalized with small molecule drugs, including camptothecin (CPT), and therapeutic oligos, such as anti-miRNA21 or siRNAs, which demonstrated significant cancer inhibition effects in various tumor-bearing animal models [24–31]. Click reactions have been used to conjugate anti-cancer drugs and targeting ligands onto RNA strands [24,32,33]. Current methods to incorporate small molecules into RNA nanoparticles include non-covalent intercalation, such as doxorubicin (DOX), and covalent conjugation, such as paclitaxel (PTX) [34]. Additionally, a new approach of incorporating an anti-cancer nucleoside analog with a defined quantity and position during RNA synthesis is presented in this study. Previous studies have demonstrated that RNA nanoparticles loaded with different anti-cancer drugs showed tumor inhibition effects in various tumor models due to the EPR effect, deformative property, and active targeting [24,35,36].

RNA molecules possess a dynamic property that is critical for their biological functions, such as catalysis in ribozymes. RNA nanoparticles also have deformative properties, which enables their prolonged tumor accumulation and fast renal excretion [7,14,37]. This is favorable for the tumor inhibition effect and low toxicity. In addition to the programmability and deformative property, RNA nanoparticles are highly hydrophilic, which can be utilized to solubilize hydrophobic drugs [24, 34]. Many anti-cancer drugs suffer from low water solubility leading to high toxicities. The hydrophilic property of RNA solubilizes the conjugated drugs in an aqueous solution, thus eliminating the toxic formulations [24,34]. Furthermore, RNA nanoparticles have demonstrated a great safety profile with low toxicity, including immune and organ toxicity in various animal trials [7,14,38].

In this study, after extensive investigation, the RNA 4WJ was identified as the optimal nanoparticle to carry small molecule drugs for cancer therapy. To carry a drug for combinational therapy requires an RNA nanoparticle to have a high melting temperature (T_m), allowing for a high drug-loading capacity without interfering with the stability of the nanoparticle. Meanwhile, the high efficiency in assembly overcomes challenges in CMC production.

SN38 has recently been tested for the treatment of colon cancer [39, 40]. Constructed RNA nanoparticles harboring SN38 were evaluated as drug delivery platforms against two cancer models including colorectal cancer (CRC) xenograft and orthotopic lung metastases of colorectal cancer. The drug payload, therapeutic effect, and pathology parameters were evaluated. Functionalized RNA nanoparticles demonstrated tumor inhibition effect in all tested tumor models demonstrating the versatility of RNA nanoparticles while no observable toxicity in biochemical and histological analysis were identified.

2. Materials and methods

2.1. Synthesis of RNA strands

All RNA strands were synthesized by ASM-800ET DNA/RNA synthesizer (Biosset) using RNA A, RNA G, 2′-Fluoro C and 2′-Fluoro U phosphoramidites (ChemGenes). 5′-Hexynyl and 2′-O-propargyl phosphoramidites (Glen Research, ChemGenes) were incorporated into RNA-ALK strands for SN38 conjugation. RNA-GEM strands were synthesized using N4-Benzoyl-2′-deoxy-5-O-DMT-2′,2′-difluorocytidine 3′-CE phosphoramidite (BOC Sciences). The sequences of all RNA strands are listed in SI table (Table S1).

Conjugation of SN38–N_3 to RNA-6-alkyne (RNA-6-ALK) strand was performed using copper(I)-catalyzed alkyne-azide cycloaddition ("Click chemistry"), as previously described [34]. RNA-6-ALK strand dissolved in diethyl pyrocarbonate-treated water (DEPC-H_2O) were thoroughly mixed with SN38–N_3 dissolved in 3:1 (v/v) dimethyl sulfoxide/tert-butanol (DMSO/t-BuOH). Freshly prepared "click solution" (a mixture of CuBr/TBTA at a 1:2 M ratio in DMSO/t-BuOH) was then added with the final molar ratio of RNA/SN38/Cu^+ at 1:15:20.

After incubation at room temperature overnight, RNA-SN38 was initially purified by ethanol precipitation with 1/10 vol of 0.3 M sodium acetate and 2.5 vol of 100 % ethanol followed by resuspension in DEPC-H_2O. RNA was subsequently purified by Ion-Pair Reverse Phase high performance liquid chromatography (HPLC) using PLRP-S 4.6 × 250 mm 300 Å column (Agilent Technologies). Fully conjugated RNA-SN38 was separated from unreacted and not fully reacted RNA-ALK strands under gradient elution with 0.1 % Triethylammonium acetate (TEAA) in H_2O as solvent A and 0.1 % TEAA in 75 % Acetonitrile (AcN) as solvent B. Fractions were collected and analyzed by PAGE and pure product were combined, dried, and resuspended in DEPC-H_2O.

Synthesized RNA strands were characterized by 16 % 8 M urea PAGE in TBE buffer (89 mM Tris base, 200 mM boric acid and 2 mM EDTA) at 200 V for 1 h. After staining by ethidium bromide (EtBr, Sigma-Aldrich) and washing, gel was visualized and analyzed by a Li-Cor Odyssey Fc imaging system.

2.2. Preparation of RNA nanoparticle

To assemble 4WJ RNA nanoparticle, four single RNA strands (A, B, C, and D) were mixed at equal molar ratio in TES buffer (50 mM Tris pH = 8.0, 50 mM NaCl, 1 mM EDTA). The mixture solution was subjected to a 1-h annealing program that starts with denaturing at 95 °C for 5 min followed by slow cooling to 4 °C over 1 h in Mastercycler (Eppendorf). 4WJ-SN38 RNA nanoparticle was generated using the same procedures with four RNA-SN38 strands. 4WJ-GEM RNA nanoparticles were assembled using four RNA-GEM strands. After annealing, RNA nanoparticles were checked by 10 % native PAGE in TBE buffer at 120 V for 1 h to check the assembly efficiency. After staining by ethidium bromide (EtBr, Sigma-Aldrich) and washing, gel was visualized and analyzed by a Li-Cor Odyssey Fc imaging system.

2.3. Size measurement by DLS

The hydrodynamic diameter and zeta potential of the RNA nanoparticles with the concentration of 10 μM in TES buffer were measured using Zetasizer Nano-ZS (Malvern Instrument) at room temperature. Size distributions were plotted with data points using GraphPad Prism.

2.4. Measurement of melting profile by thermal gradient gel electrophoresis (TGGE)

The melting profile of RNA nanoparticles in TES buffer was measured by TGGE in TBE buffer. RNA nanoparticles with a final concentration of 1 μM were subjected to 10 % native PAGE gel 100 V for 60 min with a perpendicular temperature gradient (Left to right: 39.6–79.6 ° C). After staining by EtBr and washing, gels were imaged by a Li-Cor Odyssey Fc imaging system and quantified by ImageJ.

2.5. Cell culture

HT29 cells and HT29 G-L LungM3 cells were cultured in MyCoy's 5A medium (Thermo Fisher Scientific) supplemented with 10 % fetal bovine serum (FBS) at 37 °C in humidified air containing 5 % CO_2. Mouse 4T1 cells were culture in Gibco Roswell Park Memorial Institute (RPMI) 1640 (Thermo Fisher Scientific) medium with 10 % FBS at 37 °C in humidified air containing 5 % CO_2. Mouse macrophage-like RAW

264.7 cells were cultured in DMEM (Thermo Fisher Scientific) supplemented with 10 % fetal bovine serum (FBS) at 37 °C in humidified air containing 5 % CO_2.

2.6. In vitro cell binding assay using confocal microscopy

HT29 cells were grown on glass slides in 24-well plate and cultured at 37 °C overnight. RNA nanoparticles labeled with AFDye 647 were incubated with 2×10^5 HT29 cells with a final concentration of 200 nM at 37 °C for 2 h. The cells were washed twice with PBS and fixed by 4 % paraformaldehyde (PFA). After washing with PBS, the fixed cells were stained by Alexa Fluor 488 Phalloidin (Life Technologies) for cytoskeleton and Fluoroshield Mounting Medium with DAPI (Abcam) for nucleus, respectively. The cells were then imaged and analyzed by FluoView FV3000-Filter Confocal Microscope System (Olympus Corp).

2.7. In vitro cytotoxicity by MTT assay

For the cytotoxicity study of 4WJ-SN38 RNA nanoparticles, the study was evaluated by CellTiter 96® Non-Radioactive Cell Proliferation Assay (Promega). HT29 cells were plated into 96-well plate and cultured at 37 °C overnight. The cells were then incubated with samples with different concentration in 100 μl cell medium containing 10 % FBS at 37 °C for different time point (48, 72, 96 h). After the addition of 15 μl MTT dye solution and incubation at 37 °C for 4 h, 100 μl stop solution was added to each well and incubated at room temperature overnight. The absorbance at 570 nm was measured using the Synergy 4 microplate reader (BioTek).

For the combinational chemotherapy study on SN38 with Gemcitabine using 4WJ RNA nanoparticles, 4T1 cells were plated in 96-well plate and grow overnight, respectively. Cells were incubated with samples for 48 h. CellTiter 96® Non-Radioactive Cell Proliferation Assay (Promega) was performed was performed according to manual, by adding MTT dye and incubating at 37 °C for 4 h, adding stop solution and incubating at room temperature overnight, and measuring absorbance at 570 nm by Synergy 4 microplate reader (BioTek).

2.8. In vitro apoptosis assay

The cell apoptosis was studied by FITC Annexin V Apoptosis Detection Kit (BD Pharmingen). HT29 cells were plated into 24-well plate and cultured at 37 °C overnight. The cells were then incubated with samples in 400 μl cell medium containing 10 % FBS at 37 °C for 24 h. After trypsinization, HT29 cells were washed with PBS and re-suspended in 100 μl 1 × Annexin V-FITC binding buffer. After the addition of 2 μl Annexin V-FITC and 2 μl propidium iodide (PI) and incubation at room temperature for 15 min, the cell samples were transferred to flow tubes which contained 150 μl binding buffer for fluorescence-activated cell sorting (FACS) analysis by LSR II Flow Cytometer (Becton Dickinson), and the data were analyzed by FlowJo 7.6.1 software.

2.9. In vitro cytokine induction assay

RAW 264.7 cells were plated into 24-well plates and cultured at 37 °C overnight. RNA nanoparticles and lipopolysaccharide (LPS, 5.5 μg/mL, equal amount as 100 nM 4WJ RNA nanoparticles) were each incubated with macrophage cells in 200 μl Opti-MEM cell medium (Thermo Fisher Scientific) at 37 °C for 16 h. The supernatants of cell medium were collected and frozen at −80 °C for further analysis. The TNF-α and IL-6 in diluted supernatants were measured by Mouse ELISA MAX Deluxe sets (BioLegend) following manufacturer's protocols.

2.10. Animal model preparation

2.10.1. Tumor inhibition study in colorectal cancer model
All animal procedures were performed in accordance with

Subcommittee on Research Animal Care of The Ohio State University guidelines approved by the Institutional Review Board. The protocol for this animal experiment was approved by the Institutional Animal Care and Use Committee (IACUC) of The Ohio State University. Colorectal cancer cell line HT29 (2×10^6 cells) were transplanted into nude mice (4–6 weeks old) (Charles River Laboratories). Mice with established tumor nodules were randomly divided into four groups (n = 5, biologically independent animals). Samples were intravenously administrated through IV injection with a total of 5 doses (2 mg/kg, SN38, 4WJ-SN38, 4WJ-SN38-EpCAM/body weight) every 3 days for 15 days. Tumor volume was monitored everyday by caliper, calculated as (length × width^2)/2, and mouse weight was monitored every day. On day 15, mice were sacrificed, and tumors extracted and weighted.

2.10.2. Tumor inhibition study in lung metastasis model
All animal experiments were approved by the Institutional Animal Care and Use Committee at the University of Kentucky and were conducted in accordance with guidelines issued by the National Institutes of Health for the care of laboratory animals. HT29 cells were trained to be lung tropic through initial IV injection. Lung metastases were harvested and re-injected into mice; the *in vivo* selection process which is repeated three times to develop the HT29 G-L LungM3 cell line. HT29 G-L LungM3 cell line expresses GFP signal [41,42]. NOD.Cg-*Prkdc*^{scid} *Il2rg*^{tm1Wjl}/SzJ male and female mice were injected intravenously with 1×10^6 HT29 LungM3 cells. Mice were randomly divided into PBS, 4WJ, and 4WJ-SN38-EpCAM groups (n = 5, biologically independent animals). 4WJ-SN38-EpCAM samples were administrated via IV injection at the dose of 2 mg/kg (SN38/body weight) on day 5, 8, 11, 14, 17, 20, and 23 for a total of seven injections. 4WJ samples were administrated at the same RNA concentration and frequency as the 4WJ-SN38-EpCAM group. On day 24, Lago imaging was conducted using Lago SII (Spectral Instruments Imaging, Tucson, AZ) to measure the GFP signal from the lung metastasis *in vivo*. Mice were then euthanized, and lungs were harvested for *ex vivo* Lago imaging. Mice weights of different groups were measured at day 5, 8, 11, 14, 17, 20, and 23.

3. Statistics

Each experiment was repeated at least three times with triplication for each sample tested. The results were presented as mean ± SEM, unless otherwise indicated. Statistical mean differences were evaluated using unpaired *t*-test with GraphPad software, and p < 0.05 was considered statistically significant.

4. Results

4.1. Rational design of 4WJ for high drug loading and high stability

The three-way junction (3WJ) of phi29 motor pRNA has been found to have a high thermostability and has been extensively investigated as a vehicle to carry and deliver therapeutics for cancer therapy [2,7,43–45]. However, the conjugation of eight paclitaxel molecules to the 3WJ led to the destabilization of the 3WJ/drug complex, resulting in the reduction of a T_m to 30 °C. This suggests that the pRNA 3WJ is not a suitable vehicle for the delivery of chemical drugs with a high payload [34]. To optimize the drug delivery system for the chemotherapeutics, different viral pRNA 3WJ pseudoknot from literature, including the 3WJ of phi29, M2, B103, SF5 and Ga1 [46–50] were compared for chemical drug conjugation and tested for the stability of the resulting 3WJ-drug complexes.

The previously reported 4WJ, derived from phi29-3WJ, can carry 24 chemical drugs with a stable T_m of 70–80 °C [34], while the original phi29 3WJ can only carry 8-PTX with a T_m of around 30°. The higher payload of 24 chemical drugs will enhance therapeutic efficacies. It is hoped that a higher drug payload might be achieved by increasing the length of the 3WJ sequence. However, when the size of the RNA

nanoparticles increases, healthy organ accumulation occurs due to macrophage trapping [20,38]. The Immunol response also increases [51,52]; the kidney excretion is reduced due to the kidney filtration size limit; biodistribution will not be favorable; and nanoparticle production becomes complicated with numerous component strands.

In RNA structure and folding investigation, it is commonly believed that increasing the ratio of GC content will increase the T_m and thermostability. This hypothesis was tested. While each of the pRNA 3WJs from phages phi29, M2, SF5, GA1, and B103 show very similar secondary structures, while their primary sequences are very different [46–49]. The M2 3WJ has been reported as the most stable 3WJ with the highest T_m. Therefore, the M2 was mutated through GC base pair substitution in the quest for a more stable 3WJ (Fig. 1A); However, it was found that increasing GC content led to the failure of RNA 3WJ assembly. The data showed that after increasing GC content to 3WJ, smearing and misfolding appeared. Each oligo subunit self-forms into a stronger secondary structure due to the random GC base pairing within the subunit (Fig. 1B). The high GC content of each RNA strand also lead to the formation of Quadruplexes and resulted in random GC interactions among the three strands. The self-folding of the high-GC content strands and the presence of multiple complementary sequences leads to the failure in RNA nanoparticle assembly, leading to misfolding and the failure in producing homogenous RNA nanoparticles (Fig. 1B).

The mechanism of 3WJ assembly from three component strands has been reported (Fig. 1C) [53]. It has been found that each 3WJ oligo offers eight or nine nucleotides (50 % of the 16 nucleotides) to interact with each other. First, the b-strand interacts with 50 % of the c-strand due to the lowest ΔG of the dimerization in comparison to that in a-c or a-b interaction. The generated b-c dimer creates a fork structure to recruit the a-strand, resulting in the formation of the 3WJ [53]. Similar mechanism if 3WJ formation were applied to the design of 4WJ. The 4WJ possesses four helixes that, each contain a core domain that controls the structure formation and a payload domain that is used for functionalization. The folding of the 4WJ motif might start with the generation of a helix structure between two strands, which creates two fork structures for a third strand and a fourth strand to bind with it. This principle has been applied to the design of the 4WJ with high T_m and high drug loading capacity via an alternation and screening process.

4.2. CMC production of drug-contained RNA nanoparticles

RNA nanoparticles are able to be constructed under CMC production due to defined and highly programmable in terms of size, shape, stability, stoichiometry, and modification [7,14,23,54]. The procedures for the CMC product of drug-contained RNA nanoparticles are shown in Supplementary Fig. 1. Single RNA oligo strands were generated using solid-phase synthesis that is highly controlled and produced specific products. These oligos were then used to construct RNA nanoparticles through the one-pot self-assembly [34,55,56]. 4WJ has high thermostability, which was demonstrated by its high melting and annealing
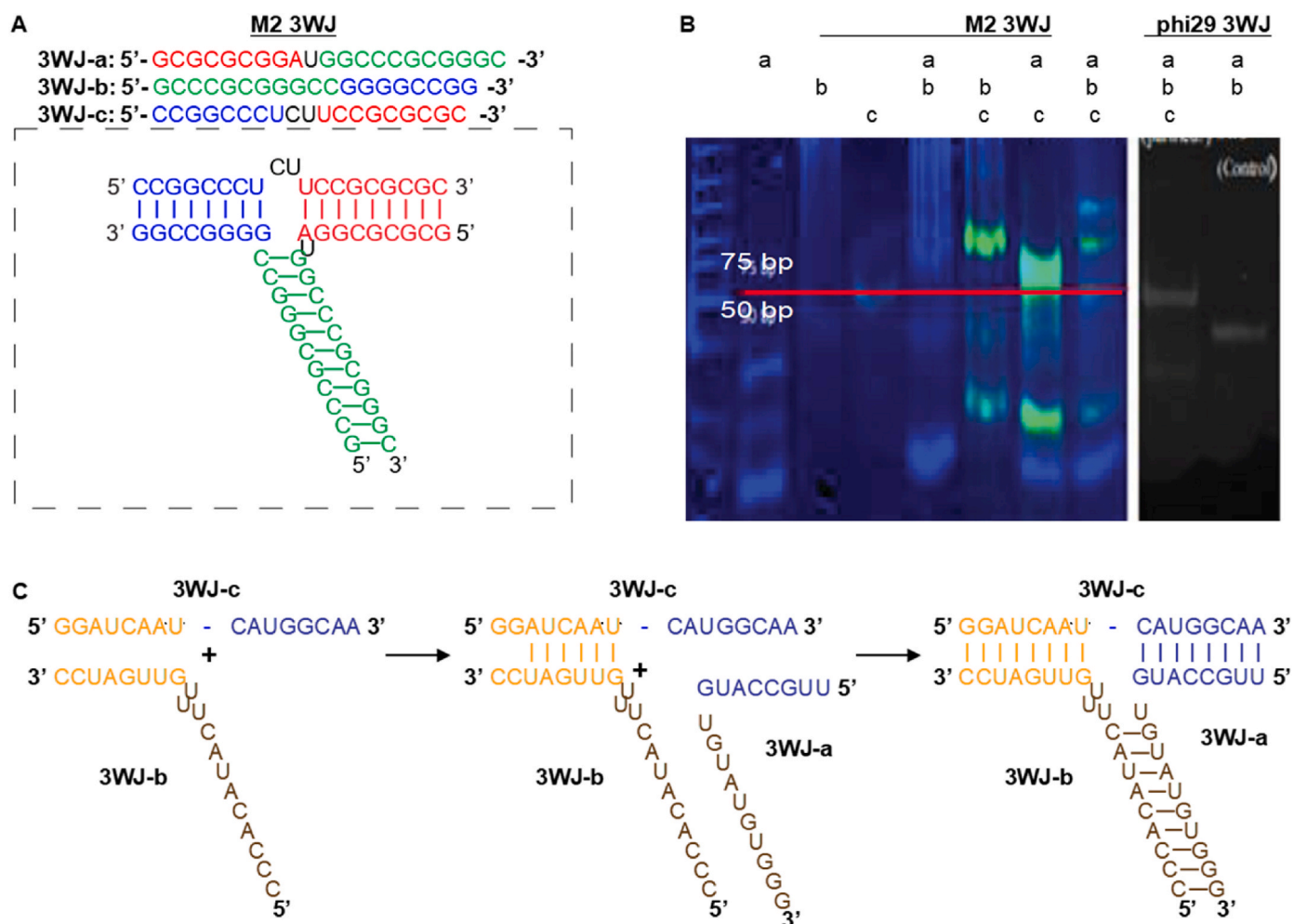

Fig. 1. The sequence and stepwise assembly of M2 3WJ. (A) The high-GC content sequence of M2 3WJ. The free energy of the thermodynamic ensemble is 60.54 kcal/mol. The frequency of the MFE structure in the ensemble is 57.16 %. (B) Gel showing the stepwise assembly of M2 3WJ and size comparison of phi29 3WJ. (C) Stepwise assembly of 3WJ.

temperature (Fig. 2E and F), thus allowing the 4WJ to carry anti-cancer drugs with high drug-loading capacity [34]. RNA strands were functionalized with a defined number of various anti-cancer drugs, including small molecule drugs such as SN38 and nucleoside analog drugs such as Gemcitabine (GEM). RNA strands with alkyne modification were synthesized and then conjugated with azide modified prodrugs such as SN38–N$_3$ (Supplementary Fig. 2). Nucleoside analog drugs were directly incorporated into the strands during the solid phase syncretization using nucleoside phosphoramidites.

4.3. Construction of functionalized thermostable 4WJ RNA nanoparticles with SN38 and EpCAM$_{apt}$

SN38 is a highly potent small molecule drug but has unfavorable pharmacokinetics due to its rapid metabolization and excretion, which limits the amount of drug reaching the disease site [57]. Various nanoparticles have been designed as the delivery platform for SN38 to extend its circulation and increase its tumor accumulation [58]. In addition, RNA nanoparticles have unique deformative properties, which allow them to penetrate through leaky blood vessels at the tumor site with better tumor accumulation compared with other types of nanoparticles [7,14,37]. Thus, a highly thermostable 4WJ RNA nanoparticle, composing four 42-nt RNA strands, A, B, C, and D, was designed as the drug delivery platform for SN38 (Fig. 2A). Each RNA strand was conjugated with 6 copies of SN38 at a three-nucleotide interval to achieve the maximal drug loading without causing steric hindrance during conjugation and aggregation after conjugation (Supplementary Figs. 3A and B). 4WJ RNA nanoparticles were self-assembled by mixing and annealing four composing RNA strands at the equal molar ratio in one-step. Both 4WJ and 4WJ-SN38 RNA nanoparticles were assembled with high efficiency demonstrated by gel electrophoresis, which indicates the drug conjugation did not interfere with the assembly (Fig. 2B). With the attachment of SN38, the size of 4WJ increased from 10.13 nm to 12.19 nm which demonstrates no aggregation of conjugated SN38 in water (Fig. 2C). In addition, the drug conjugation did not affect the negative charge of 4WJ RNA nanoparticles (Fig. 2D). 4WJ RNA

nanoparticles were designed with high thermostability through the incorporation of 2′F–C and U as well the high GC content to overcome impacts of drug conjugation. The annealing curve showed that both 4WJ and 4WJ-SN38 exhibited high thermostability, with the annealing temperature (T$_a$) above 80 °C, which is much higher than physiological condition (37 °C) (Fig. 2E). The TGGE gel further demonstrated the high thermostability of 4WJ-SN38 with the T$_m$ higher than 80 °C (Fig. 2F).

Additionally, RNA aptamers are single-stranded RNA with a defined folding structure that are capable of binding to target molecules with high affinity and selectivity [59]. RNA 4WJ nanoparticles were constructed with epithelial cell adhesion molecule (EpCAM) RNA aptamers (EpCAM$_{apt}$) to instill specific tumor targeting [28] (Fig. 2A). EpCAM has been found to be overexpressed in numerous cancers, including colorectal cancer [60], and provides a good biomarker and cell surface receptor for targeting of RNA nanoparticles. Therefore, a well published and proven EpCAM$_{apt}$ was placed onto the a helical branch of the 4WJ through sequence through extending B strand during synthesis without additional conjugation and purification steps [61]. Resulting RNA nanoparticles demonstrated homogenous products by PAGE analysis (Fig. 2B) and the inclusion of the EpCAM$_{apt}$ should provide selective binding to tumor expressed EpCAM for receptor mediated endocytosis.

Improvement of poor drug water-solubility by covalent conjugation to RNA strand: a case study on SN38.

Many chemotherapeutics suffer from poor water solubility and are highly hydrophobic thus limiting their pharmaceutical formulations, including SN38 [62]. To solve this solubility issue, we designed RNA-SN38 conjugates taking advantage of the highly hydrophilic property of RNA. The multivalency of RNA enables the high drug loading capacity and precise control over the amount of modification. Multiple copies of hydrophobic SN38 were conjugated to hydrophilic RNA strands with defined stoichiometry as described above (Supplementary Figs. 2 and 3). The conjugation resulted in a significant improvement of its water solubility as demonstrated by UV/Vis spectrometry and visual observation. Dissolving RNA-6-SN38 conjugate in DEPC water yield clear solutions at increasing concentration from 12.5 μM to 800 μM (4.9–313.9 μg/mL) (Supplementary Fig. 3C). The
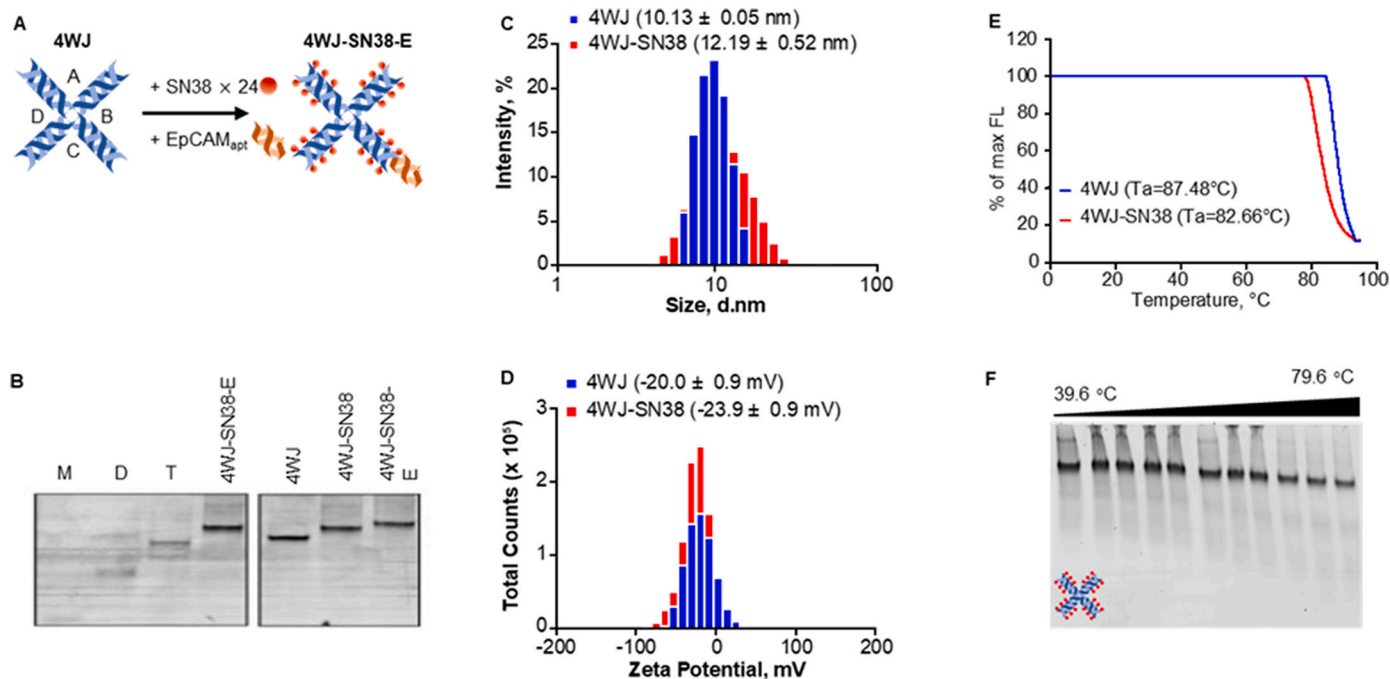

Fig. 2. Assembly and characterization of 4WJ-SN38-Epcam (4WJ-SN38-E) RNA nanoparticles. (A) Schematic of functionalizing 4WJ RNA nanoparticles with 24 copies of SN38 and one copy of EpCAM RNA aptamer. (B) Gel showing the stepwise assembly of 4WJ-SN38-E (M: monomer, D: dimer, T: trimer) and size comparison of 4WJ, 4WJ-SN38, and 4WJ-SN38-E. (C) Size distribution of 4WJ and 4WJ-SN38. (D) Zeta potential distribution of 4WJ and 4WJ-SN38. (E) Thermostability of 4WJ and 4WJ-SN38 demonstrated by annealing profile. (F) Thermostability of 4WJ-SN38 demonstrated by melting profile.

absorbance of free SN38 in water remains at low level within the measured concentration range, which suggests the extremely poor water solubility of SN38. In contrast, the absorbance of RNA-SN38 in water showed linear increase with concentration which indicates that RNA-SN38 was completely dissolved water (Supplementary Fig. 3C). The solubility of RNA-SN38 in water is comparable to the solubility of free SN38 in DMSO, a common solvent for SN38, as indicated by the similar proportional increase of absorbance as a function of concentration. And the comparison of the clear solution of RNA-6-SN38 versus the cloudy suspension of SN38 in water at high concentration (313 μg/mL, 800 μM) further proved the improvement of water solubility after conjugation (Supplementary Fig. 3C). Collectively, the water solubility of SN38 was increased by at least 60-fold after conjugation to RNA, compared to the reported solubility of free SN38 (5 μg/mL, 12.7 μM) and its prodrug, irinotecan, (10^7 μg/mL, 182.4 μM) in water.

4.4. In vitro cell binding and internalization of SN38 RNA nanoparticles mediated by the EpCAM aptamer

Specificity is one of the key considerations in the drug delivery field. Targeted delivery can not only improve therapeutic outcome but also reduce the accumulation in normal organ and tissue, thus lowering side effects. EpCAM is expressed at low levels in normal epithelial tissues but highly expressed in 70–90 % of carcinomas such as colorectal cancer cells [60]. To evaluate the specific targeting efficiency, AFDye 647 was attached to RNA nanoparticles as a fluorescent indicator. HT29 cells were incubated with 4WJ RNA nanoparticles which were then imaged by confocal microscope. 4WJ RNA nanoparticle itself showed limited observable binding to HT29 cell membranes due to its negative charge repulsion from the cell membrane. No enhanced RNA signal within the cell cytoplasm was not observed. However, as is shown in the 4WJ-SN38-EpCAM group, the red signal from the RNA nanoparticles is distributed on the membrane at different levels. Some area has a very high RNA signal distribution, and we believe it was due to EpCAM RNA aptamer binding to EpCAM on the cell membranes. We can also observe the enhanced RNA signal within the cell cytoplasm, as 4WJ-SN38-Ep-CAM RNA nanoparticles showed overlap of red signals from RNA nanoparticle and green signals from cytosol. It may indicate that RNA exists in the endosome after Aptamer-EpCAM mediated internalization (Fig. 3A). These results together demonstrated that EpCAM$_{apt}$ displaying RNA nanoparticles specifically bind to EpCAM-overexpressed tumor cells and are further internalized into the cells efficiently by receptor-mediated endocytosis. The enhanced internalization profile provides a foundation for 4WJ-SN38-EpCAM to be applied in CRC targeting and therapy.

4.5. In vitro cytotoxicity and immunogenicity of SN38 RNA nanoparticles

To determine the cytotoxicity of RNA-SN38 nanoparticles, dose-dependent MTT assay with different incubation time was performed. The cell viability results show that 4WJ RNA nanoparticle has no observable toxicity within the tested concentrations (0.025–1 μM) and time points (48, 72, 96 h), which indicates its safety to be used as a delivery platform (Fig. 3B). However, 4WJ-SN38-EpCAM RNA nanoparticle inhibited HT29 cell growth in a concentration dependent manner which demonstrated that SN38 was released from the RNA nanoparticles and retained its pharmacological activity to inhibit tumor cell growth. Interestingly, the cytotoxicity of 4WJ-SN38-EpCAM was relatively lower at 48 h but became the same at 96 h in comparison to free SN38, which suggests that SN38 is gradually released from RNA nanoparticles. Another explanation is that 4WJ-SN38-EpCAM internalization may take a longer time compared to the free SN38. To further confirm the inhibitive effect, PI and FITC Annexin V double staining analysis was performed. Consistent with the MTT assay, 4WJ RNA nanoparticles induced no observable apoptotic effect while 4WJ-SN38-EpCAM induced 31.6 % of cells which is similar to the 38.0 % induced

by SN38 (Fig. 3C).

Special formulations such as Cremephor EL/Ethanol have been used to dissolve hydrophobic drugs such as paclitaxel for cancer treatment [63]. However, these formulations could induce undesirable immune responses. Immunogenicity is also a concern for the use of nanoparticles fabricated with biomaterials. RNA nanoparticles are highly biocompatible and has no or low immune response with careful sequence design [13,51]. To evaluate the immunogenicity of 4WJ RNA nanoparticles, production of pro-inflammatory cytokines, including TNF-α (tumor necrosis factor α) and IL-6 (interleukin-6) was investigated *in vitro*. TNF-α is cytokine involved in systemic inflammation and one of the cytokines that make up the acute phase reaction [64]. IL-6 is an interleukin that acts as both a pro-inflammatory cytokine and an anti-inflammatory myokine, which is secreted to stimulate immune response during infection [65]. The ELISA results showed that both bare 4WJ and functionalized 4WJ-SN38-EpCAM at the therapeutic concentration (100 nM) induced negligible TNF-α nor IL-6 production compared to LPS (lipopolysaccharide) positive control while incubating with mouse macrophage like RAW 264.7 cells [66] (Fig. 5A and B). The low induction of cytokine suggests that RNA is a biocompatible and relative safe biomaterial.

4.6. Synergistic effect of SN38 with GEM achieved by RNA nanoparticles

Combinational chemotherapy is commonly used for cancer treatment to increase the therapeutic outcome by achieving additive and synergistic effects and preventing drug resistance related to monotherapy [67]. RNA nanoparticles offer a great platform to combine multiple anti-cancer drugs with distinct physicochemical and pharmacokinetic profiles due to their multivalency [68]. Moreover, the programmability of RNA nanoparticles enables them to precisely control the ratio incorporated drugs, which is crucial for reaching maximal enhanced therapeutic effect.

Here, we investigated the combination therapy of SN38 with Gemcitabine, which is a nucleoside analog drug. RNA-SN38 strands were mixed with RNA strands including GEM to achieve combinational therapies. 4WJ RNA nanoparticles with GEM: SN38 ratio at 1 : 3 and 1 : 2 were constructed using different RNA-GEM and RNA-SN38 strands and were used for cytotoxic study (Fig. 4). 4WJ-GEM-SN38 (1:3) demonstrated improved cytotoxicity compared to 4WJ-GEM (Fig. 4A). Interestingly, 4WJ-GEM-SN38 (1:2) demonstrated improved cytotoxicity compared to 4WJ-GEM at a low concentration range while showed better cytotoxicity compared to 4WJ-SN38 at a high concentration range (Fig. 4B). The cell viability data was used to generate dose response matrix. A study was conducted between 4WJ-GEM and 4WJ-SN38, which showed good synergistic effect with an HSA synergy score of 11.693 (Fig. 4C and D).

4.7. In vivo colorectal tumor inhibition by 4WJ-SN38-EpCAM

Given the demonstration of specific tumor cell binding, high apoptotic effect, and negligible immune response, we performed the tumor suppression study in CRC tumor xenograft model. The therapeutic effect of 4WJ-SN38-EpCAM nanoparticles was validated by a tumor inhibition study in an HT29 xenografic model in nude mice. After tumors grew to approximately 50 mm³, mice bearing HT29 xenograft were randomly divided into four groups of PBS, SN38, 4WJ-SN38, and 4WJ-SN38-EpCAM. Samples were administrated via intravenous injection (IV) at the dose of 2 mg/kg (SN38/body weight) on day 0, 3, 6, 9, and 12 for a total of five injections. Both the tumor growth curve and the tumor weight comparison demonstrated 4WJ-SN38-EpCAM has significant tumor suppression in comparison to PBS group (Fig. 5C). Both RNA-SN38 nanoparticles did not cause any fatality or obvious weight changes during experiments, which suggests a favorable safety profile of the RNA-SN38 nanoparticles. Due to the recognition between EpCAM aptamer and its overexpressed receptor on HT29 cells, 4WJ-SN38-
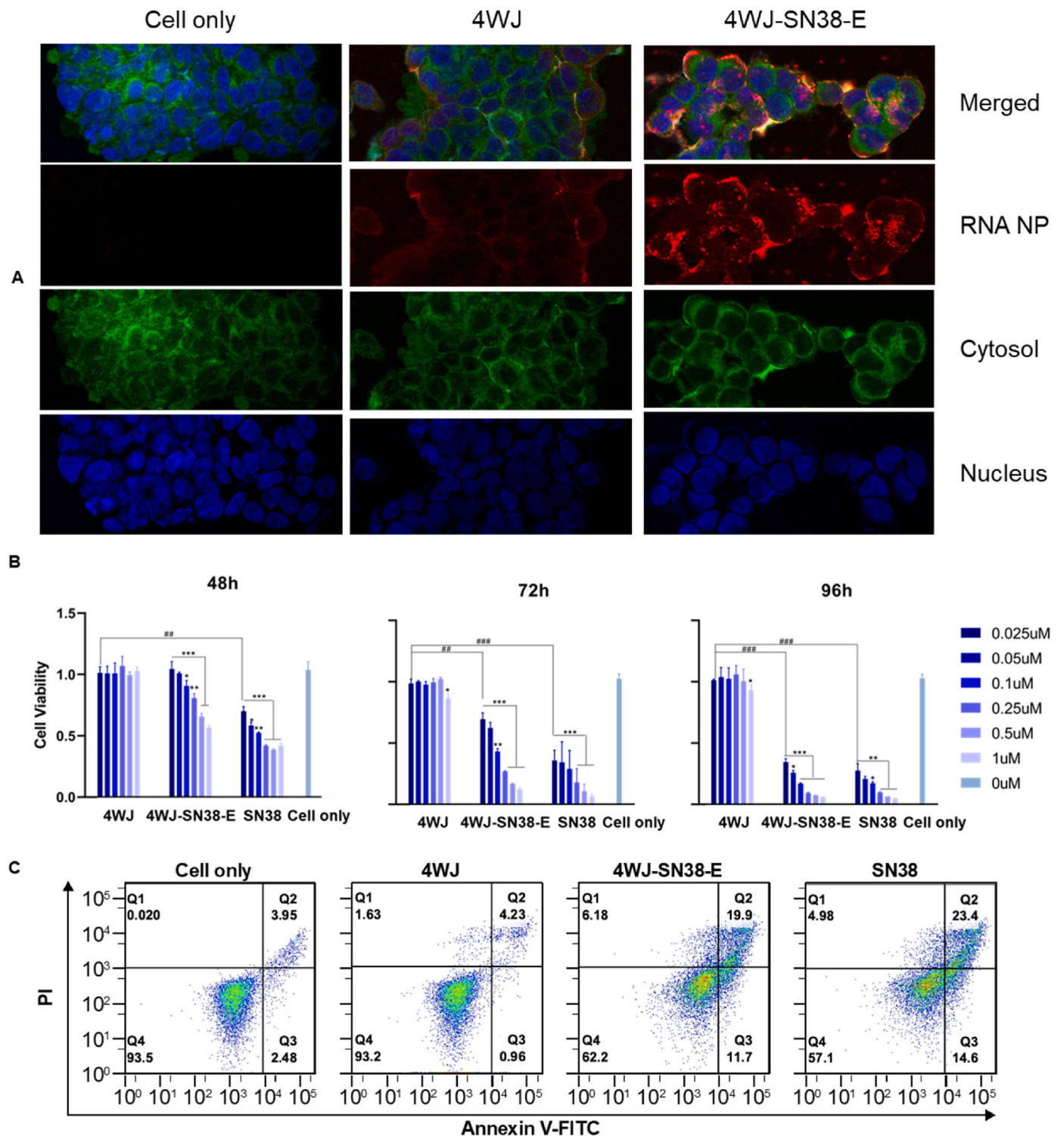
Fig. 3. *In vitro* cell binding, internalization, and cancer suppression study of 4WJ-SN38-E RNA nanoparticles. (A) Confocal images of HT29 cells after incubation with PBS, 4WJ, and 4WJ-SN38-E, respectively. (Blue: nucleus; Green: Cytosol; Red: RNA nanoparticle). (B) Evaluation of cell viability by MTT assay in HT29 cells incubated with RNA nanoparticles and SN38 for 48, 72, and 96 h, respectively. Statistics were calculated by two-tailed unpaired *t*-test presented as mean ± SEM. Significant results compared to the RNA nanoparticle at a concentration of 0.025 μM are marked with an asterisk (*$p < 0.05$, **$p < 0.01$, ***$p < 0.001$). Significant results compared to the 4WJ at a concentration of 0.025 μM are marked with an hash (##$p < 0.01$ and ###$p < 0.001$). (C) *In vitro* apoptotic effects of RNA nanoparticles and SN38 by PI/Annexin V-FITC dual staining and FACS analysis (Q2 = Annexin V-FITC positive & PI positive, indicating late apoptotic and dead cells; Q3 = Annexin V-FITC positive & PI negative, indicating early apoptotic cells). (For interpretation of the references to color in this figure legend, the reader is referred to the Web version of this article.)
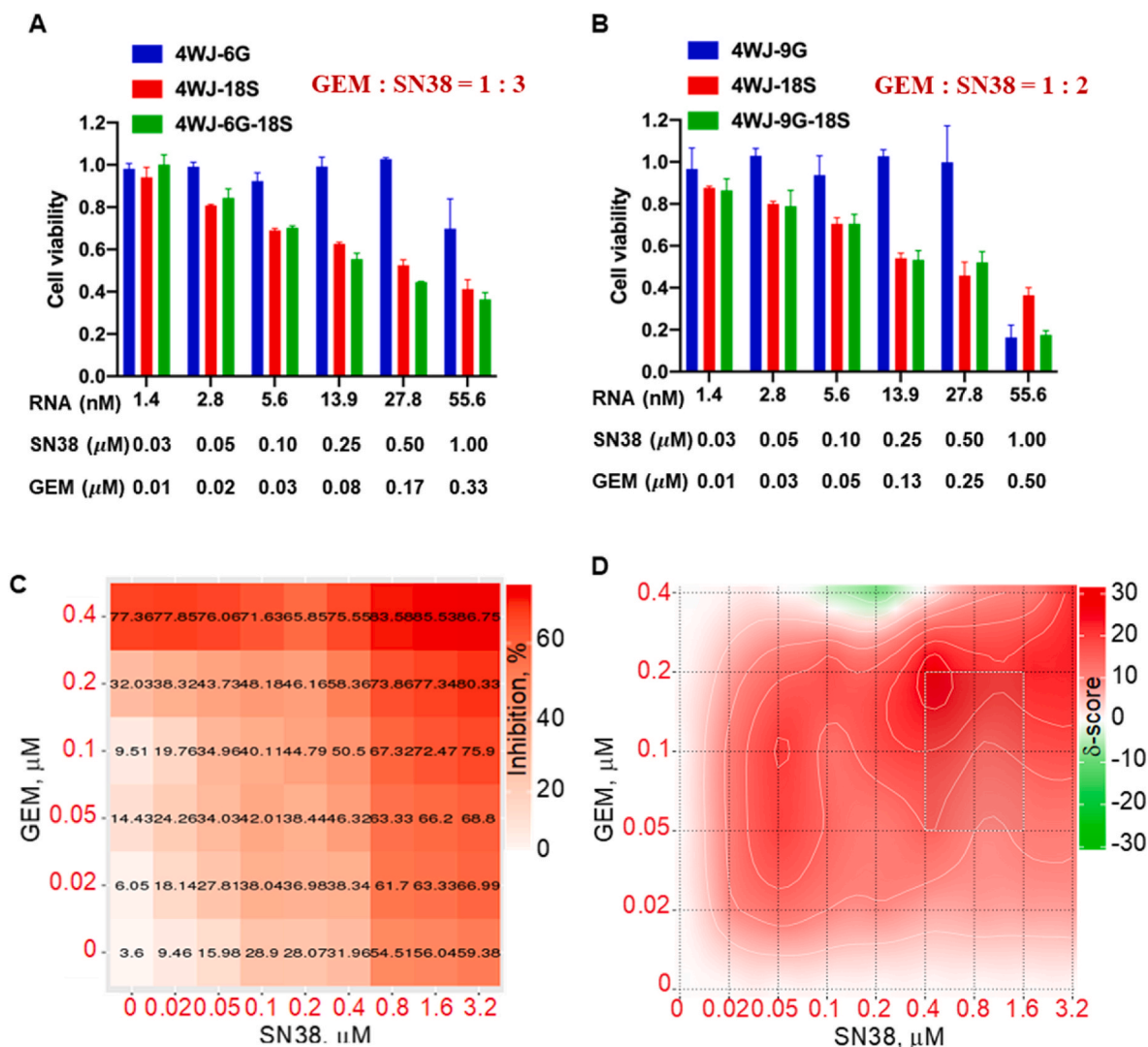
Fig. 4. Combinational chemotherapy of SN38/GEM achieved by 4WJ RNA nanoparticles. (A,B) Cytotoxicity of 4WJ-GEM-SN38 with 1 : 2 and 1 : 3 ratio of GEM: SN38. (C) Dose-response matrix of 4WJ-GEM/SN38 and (D) HSA synergy map of 4WJ-GEM/SN38.

EpCAM outperformed 4WJ-SN38 in tumor suppression by about 20.37 % more reduction in tumor weight (Fig. 5D).

4.8. *In vivo colorectal cancer lung metastasis inhibition by 4WJ-SN38-EpCAM*

The therapeutic effect of 4WJ-SN38-EpCAM nanoparticles was further validated by a tumor inhibition study in a colorectal cancer lung metastasis model. Five days after IV injection of lung metastatic trained HT29 cell lines with GFP protein expression, Lago imaging was conducted to verify the existence of lung metastasis (Fig. 6A).

Compared to PBS group, 4WJ nanoparticle control, 4WJ-SN38-EpCAM shows significant inhibition on the colorectal cancer lung metastasis both *in vivo* and *ex vivo* as verified by the decreased GFP protein expression (Fig. 6B and C). Meanwhile, 4WJ-SN38-EpCAM treatment did not cause any fatality, and the mouse weight shown no significant change in 4WJ-SN38-EpCAM treatment group compared to the decreased weight among all other three groups (Fig. 6D). All data show enhanced therapeutic efficacy and a limited toxicity profile of 4WJ-SN38-EpCAM treatment against the CRC lung metastasis.

5. Discussion

Since its inception in 1998 [69], the field of RNA nanotechnology has quickly grown into a viable drug delivery vehicle that offers many benefits such as improved pharmacological parameters, avoidance of healthy organs for low toxicities, rapid renal clearance, and high spontaneous tumor accumulation [7,14]. Research has found that RNA nanoparticles are mobile and deformable, which can enhance passage through the tumor vasculature and be quickly excreted through the kidneys, thereby avoiding remaining in healthy organs and causing toxicity [37]. Additionally, RNA nanoparticles have been shown to specifically bind and target various cancers through the inclusion of chemical or RNA-targeting ligands [24–28,34–36,70–72]. Their multivalent nature allows for easy modification with several functional groups, and high thermostability allows for stable conjugation of ligands or therapeutic groups [14,36,55,73].

We have carried out extensive studies to search for the best RNA structures to carry drugs for cancer treatment. We found that the 4WJ is the optimal nanocarrier in cancer treatment [34]. This is due to the special sequence design at the 4WJ-core center [34]. It is generally believed that increasing the GC content of 3WJ might be a suitable method to increase the T_m of RNA nanoparticles. However, we found that increasing GC content (Fig. 1A) leads to the failure of the formation
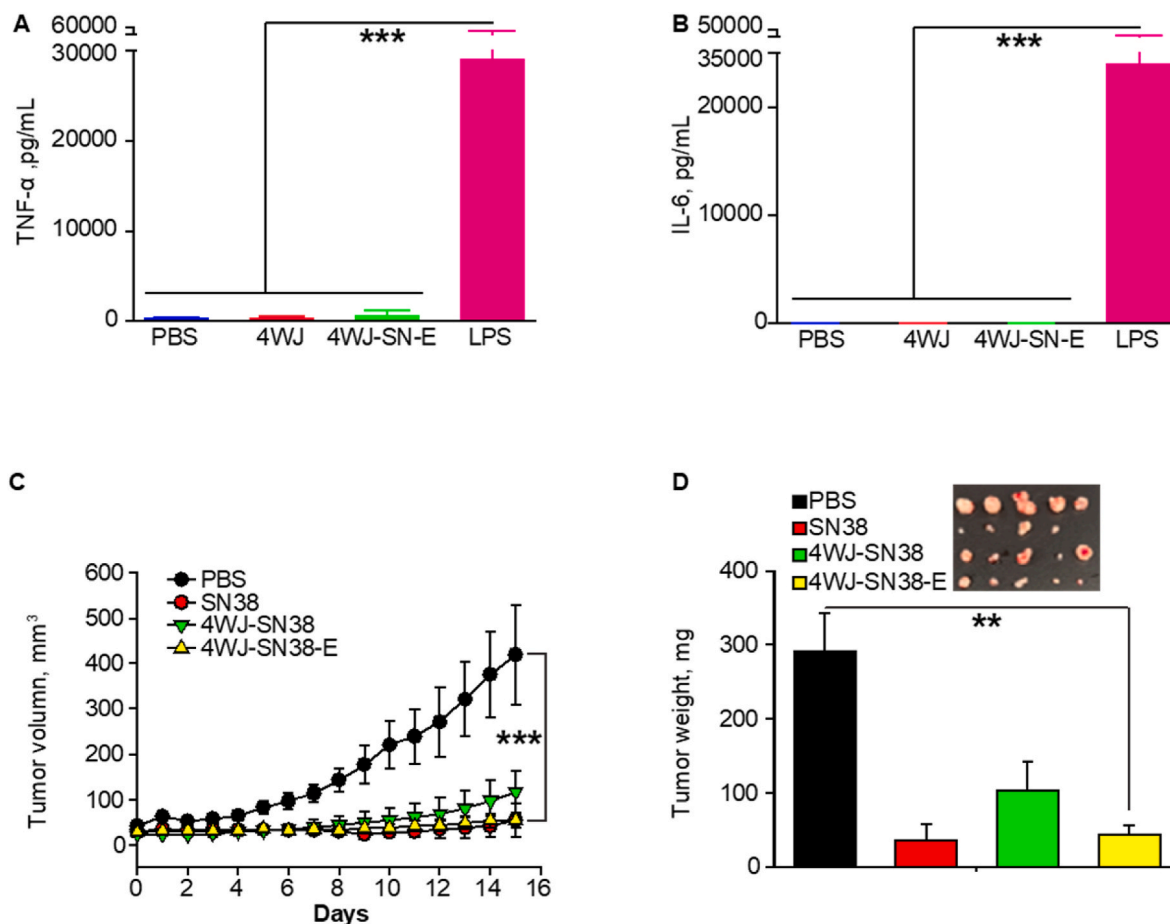
Fig. 5. *In vitro* immune response and *in vivo* tumor inhibition of 4WJ-SN38-E RNA nanoparticles. (A,B) Evaluation of TNF-α (A) and IL-6 (B) production after incubating 4WJ-SN38-E with macrophage-like cells by ELISA. (C) Intravenous treatment of nude mice bearing HT29 xenografts with 4WJ-SN38-E and control groups every three days for a total of 5 injections (indicated by arrows). Mice tumor size was monitored during the time course of treatments. (D) Comparison of tumor weight and size at the endpoint (n = 5 biologically independent animals). Statistics were calculated by two-tailed unpaired *t*-test presented as mean ± SEM, **p < 0.01, ***p < 0.001.

of the RNA 3WJ structure (Fig. 1B). The GC pairing undergoes a specific hydrogen bonding with each other. In theory, each GC base pair is held together by three hydrogen bonds, which is more stable than the AU base pair which only holds two hydrogen bonds. Our data showed that after increasing GC content in the 3WJ structure (Fig. 1A), all the smears and misfolding showed the fact that GC pairs are easier to form an incorrect secondary structure of each RNA strand (Fig. 1B). High GC content can also lead to the formation of a Quadruplex [74]. The study clearly showed that single strands a, b, and c led to the formation of self-binding dimers (Fig. 1C) that migrate much slower than the desired 3WJ single strands, resulting in multiple unwanted RNA pairings bands on the gel. It is also found that an increase of GC base pair can significantly increase the chance of the mispairing of RNA double helix between two stands of 3WJ before the formation of 3WJ RNA structures. Meanwhile, when the strands a, b, and c with high GC content were mixed with an equal molar concentration, multiple bands were found instead of a single band. In conclusion, as a general criterion in RNA nanotechnology that requires inter-strand interactions, it is not always feasible to increase GC content to enhance the rate of hybridization to increase T_m [75–77].

As a supplement to the advantage of 4WJ-RNA nanoparticles, 4WJ can carry 24 copies of chemical drugs, and its T_m is 70–80 °C [34]. Our previously published 3WJ can only carry 10 copies of paclitaxel, and the T_m is around 30 °C [34]. The high payload of chemical drugs will enhance the therapeutic efficacy. With a T_m of 30 °C, the 3WJ-drug complex will dissociate in the human body that holds a normal temperature of 37 °C. However, 4WJ will not dissociate because of its higher T_m. Thus, 4WJ with 24 copies of chemical drugs with a T_m of 70–80 °C is more appropriate for *in vivo* application. The size of nanoparticles is another critical parameter for *in vivo* biodistribution. The 4WJ RNA nanoparticle with a size of 10 nm [1,34,37] is a favorable size for biodistribution. When the particles are larger than 4WJ, stronger healthy organ accumulation will occur due to the capture of macrophages. The renal excretion rate will also be reduced due to renal filtration limitations, and the biodistribution will be unfavorable. The production and purification process during CMC production will be more complicated due to the production efficacy in solid-phase synthesis.

Here we demonstrate the versatility of 4WJ nanoparticles to harbor numerous copies of small molecule drugs and nucleoside therapies, including SN38 and GEM. The 4WJ RNA nanoparticle is easily adaptable to accept different drugs and combinations of drugs while remaining stable. The conjugation of these therapeutics results in several benefits including solubilization of hydrophobic therapeutics (Supplementary Fig. 3), specific delivery to tumors (Figs. 3A, 5 and 6), avoidance of immune responses (Fig. 5), controlled release in tumor microenvironments (Figs. 5 and 6) while remaining safe and presenting no toxicities [78].

The novelty of the presented RNA nanoparticle platform is its ability to easily adapt to the treatment of various cancers. 4WJ RNA nanoparticles can target and significantly inhibit colon cancer growth. Most notably, 4WJ RNA nanoparticles can target and almost completely
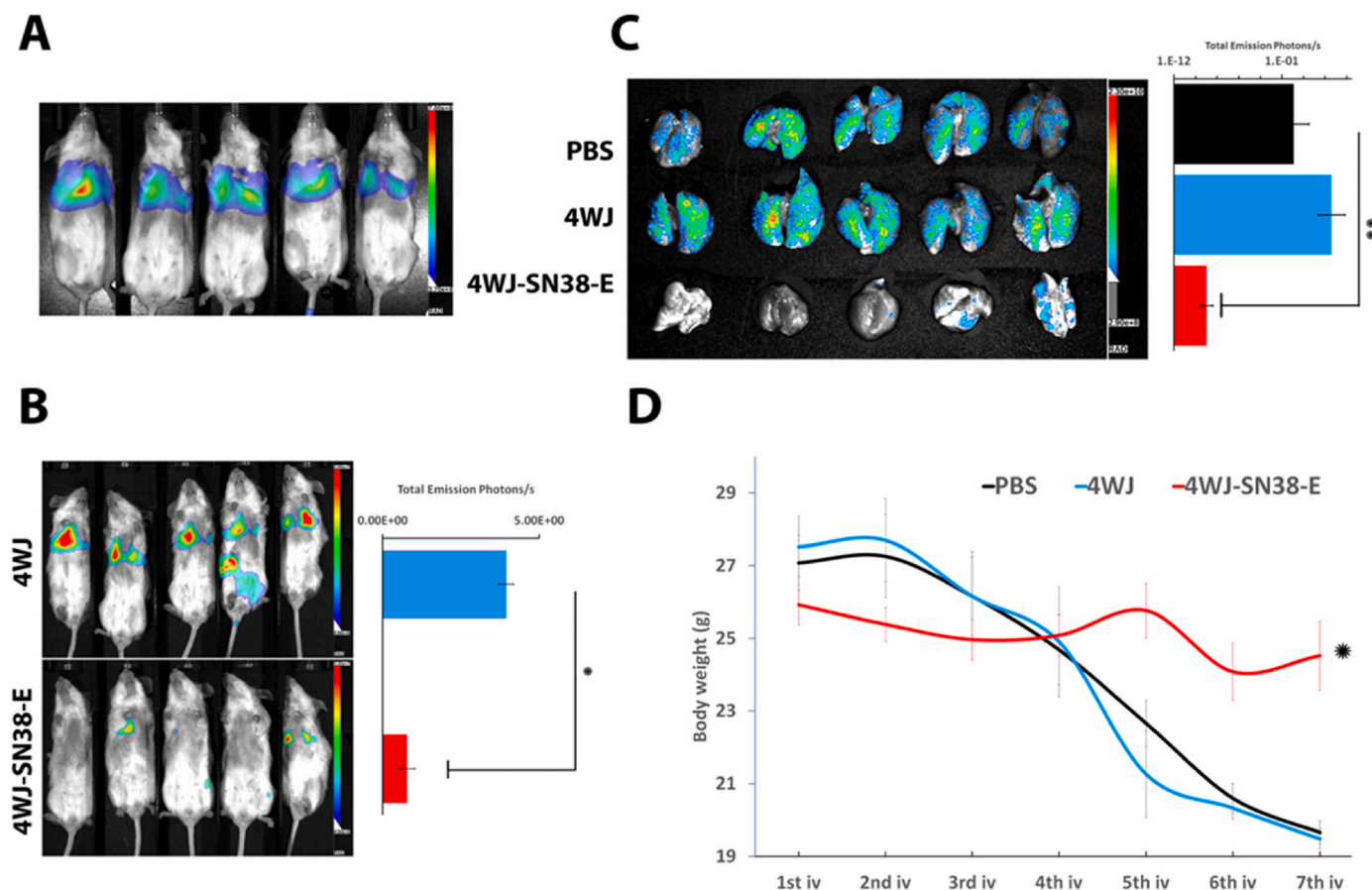
Fig. 6. *In vivo* colorectal cancer lung metastasis model inhibition of 4WJ-SN38-E. (A) Lago imaging to confirm metastasis establishment 5 days after IV injection. (B) Bioluminescence to compare metastasis *in vivo* between 4WJ and 4WJ-SN38-E groups. The mice in the PBS control group were so sick (see D) and cannot survive till the whole body imaging. (C). GFP imaging to compare metastasis *ex vivo* between PBS, 4WJ, and 4WJ-SN38-E groups. (D). Mice weight changes on day 5, 8, 11, 14, 17, 20, and 23.

inhibit CRC metastasis in mouse lungs. This provides a platform for future RNA therapeutic development by simply changing drug conjugates on the nanoparticle to match clinically relevant therapies to each tumor subtype. Taken together, RNA nanotechnology is a powerful new drug development platform for treating various cancers. Due to its safety, efficacy, and specificity, it is expected to be rapidly translated into clinical treatments.

Clinical translation is another main topic of this research since it is an important intermediate step to bridge fundamental and application research. This translational application research follows the advancements in our fundamental research in the RNA field. We use our reported RNA/drug 4WJ complex with defined structure, shape, size, stoichiometry, ligand, and payload, together with controlled drug release (Fig. 2) [25,34,79]. We have also proven our RNA nanoparticle to 1) remain stable in *in vivo* environments while harboring multiple chemical drugs for efficacious delivery, 2) accumulate at high levels in tumors, and provide active targeting by RNA aptamers for the efficient treatment of tumor and metastases, and 3) demonstrate safety with no damage to healthy organs or induction of cytokines or immune responses [25,34]. These studies are the basis for further clinical translation.

In a recent study [78] focused on assessing the safety of RNA nanoparticles, our *in vitro* testing of these materials revealed no signs of hemolysis, platelet aggregation, complement activation, plasma coagulation, interferon induction, or cytokine secretion, following the established protocols of the nanotechnology characterization laboratory [80–86]. Additionally, when examining the histology of RNA nanoparticles loaded with chemotherapy drugs, no organ toxicity was observed, and there were no changes in serum biochemical or hematological markers in *in vivo* tests. In contrast, when comparing to free chemotherapeutic drugs like SN38 at equivalent concentrations, it was evident from animal experiments that there was notable hepatotoxicity, as indicated by increased levels of glutamate oxalyl acetate aminotransferase and glutamic acid pyruvate aminotransferase in the serum. Furthermore, our animal model data demonstrated a significant reduction in white blood cell count, platelet count, and heme concentration in the free SN38 treatment group [78], underscoring the safety benefits of utilizing RNA nanoparticles as carriers for chemotherapy drugs.

In sum, RNA nanotechnology has generated stable nanoparticles capable of delivering therapeutics, such as anti-miRNA, siRNA, and small molecule drugs, to tumors in a safe and targeted manner, without causing any toxicity or affecting healthy organs through non-selective delivery [8,11,35,69,87–103]. Recent progress has shown that RNA nanoparticles can: 1) exhibit diverse characteristics; 2) create structures with precise control over shape, size, and composition; 3) self-assemble spontaneously; 4) maintain stability in terms of thermodynamics, chemistry, and enzymatic activity. Recent FDA approval of COVID-19 mRNA vaccines (utilizing the capping enzyme by Guo [104]) and RNA drugs *Onpattro*, *Oxlumo*, and *Givlaari* [105–107] demonstrates RNA nanotechnology is poised to move to the clinic. RNA nanotechnology is an analog of "LEGO" [37,101,108,109], and the novelty of the proposed RNA nanoparticle platform lies in its ability to be applied clinically to the treatment of various cancers [1,13,110–114].

6. Conclusions

The rational design of branched 4-way junction (4WJ) RNA nanoparticles has been employed to achieve exceptional thermal stability. This enhanced stability allows for the delivery of substantial drug payloads, particularly for the treatment of cancer, including metastatic tumors in the lungs. The 4WJ RNA nanostructures harboring anticancer drug SN38, display remarkable versatility in inhibiting two distinct color cancer models, including a xenograft and orthotopic lung metastasis. The resulting 4WJ RNA/SN38 complex exhibits a capacity to target cancer cells spontaneously and effectively. When an RNA aptamer ligand was added, a specificity increased. Furthermore, the 4WJ structure demonstrates swift renal excretion, rapid clearance from the body, minimal organ accumulation, and exhibits no detectable signs of toxicity or immunogenicity. The assessment of safety parameters has been carried out through organ histology, blood biochemistry, and pathological analysis. With its high efficiency in inhibiting cancer, negligible drug toxicity, and favorable production characteristics, RNA nanoparticles like 4WJ hold significant promise for translation into a valuable drug candidate in cancer therapy.

Author contributions

Conceptualization, P.G. and Y.S.; Methodology, X.L., W.J.L., Y.C.L., L.C.C., and K.J.; Investigation, X.L., W.J.L., Y.C.L and P.R.; Writing - Original Draft, X.L., K.J., T.C.C., W.J.L., and P.G.; Writing - Review & Editing, K.J., M.P., Y.S.H., and P.G.; Visualization, X.L., K.J., W.J.L., and P.G.

Funding

Declaration of competing interest

P.G. has patents P2024-136-8471 and P2022-263-8315 pending to The Ohio State University. P.G. is the consultant, licensor, and grantee of Oxford Nanopore Technologies; as well as the cofounder and consultant of ExonanoRNA, LLC. Other authors declare that they have no known competing financial interests or personal relationships that could have appeared to influence the work reported in this paper.

Data availability

Data will be made available on request.

Acknowledgements

Appendix A. Supplementary data

Supplementary data to this article can be found online at https://doi.org/10.1016/j.biomaterials.2023.122432.

References

[1] P. Guo, The emerging field of RNA nanotechnology, Nat. Nanotechnol. 5 (12) (2010) 833–842.

[2] Y. Shu, F. Pi, A. Sharma, M. Rajabi, F. Haque, D. Shu, M. Leggas, B.M. Evers, P. Guo, Stable RNA nanoparticles as potential new generation drugs for cancer therapy, Adv. Drug Deliv. Rev. 66 (2014) 74–89.

[3] M.J. Mitchell, M.M. Billingsley, R.M. Haley, M.E. Wechsler, N.A. Peppas, R. Langer, Engineering precision nanoparticles for drug delivery, Nat. Rev. Drug Discov. 20 (2) (2021) 101–124.

[4] M. Chandler, B. Johnson, E. Khisamutdinov, M.A. Dobrovolskaia, J. Sztuba-Solinska, A.K. Salem, K. Breyne, R. Chammas, N.G. Walter, L.M. Contreras, P. Guo, K.A. Afonin, The International Society of RNA nanotechnology and nanomedicine (ISRNN): the present and future of the Burgeoning field, ACS Nano 15 (11) (2021) 16957–16973.

[5] K.A. Afonin, M.A. Dobrovolskaia, W. Ke, P. Grodzinski, M. Bathe, Critical review of nucleic acid nanotechnology to identify gaps and inform a strategy for accelerated clinical translation, Adv. Drug Deliv. Rev. 181 (2022), 114081.

[6] D. Shu, W.D. Moll, Z. Deng, C. Mao, P. Guo, Bottom-up assembly of RNA Arrays and Superstructures as potential parts in nanotechnology, Nano Lett. 4 (9) (2004) 1717–1723.

[7] D.W. Binzel, X. Li, N. Burns, E. Khan, W.J. Lee, L.C. Chen, S. Ellipilli, W. Miles, Y. S. Ho, P. Guo, Thermostability, Tunability, and Tenacity of RNA as Rubbery Anionic Polymeric materials in nanotechnology and nanomedicine-specific cancer targeting with undetectable toxicity, Chem. Rev. 121 (13) (2021) 7398–7467.

[8] Y.H. Roh, J.Z. Deng, E.C. Dreaden, J.H. Park, D.S. Yun, K.E. Shopsowitz, P. T. Hammond, A Multi-RNAi Microsponge platform for simultaneous controlled delivery of multiple small interfering RNAs, Angew. Chem., Int. Ed. Engl. 55 (10) (2016) 3347–3351.

[9] D.L. Jasinski, D.W. Binzel, P. Guo, One-pot production of RNA nanoparticles via Automated processing and self-assembly, ACS Nano 13 (4) (2019) 4603–4612.

[10] S.L. Sparvath, C.W. Geary, E.S. Andersen, Computer-aided design of RNA origami structures, Methods Mol. Biol. 1500 (2017) 51–80.

[11] H.C. Hoiberg, S.M. Sparvath, V.L. Andersen, J. Kjems, E.S. Andersen, An RNA origami Octahedron with Intrinsic siRNAs for potent gene knockdown, Biotechnol. J. 14 (1) (2019), e1700634.

[12] M.N. Bui, M. Brittany Johnson, M. Viard, E. Satterwhite, A.N. Martins, Z. Li, I. Marriott, K.A. Afonin, E.F. Khisamutdinov, Versatile RNA tetra-U helix linking motif as a toolkit for nucleic acid nanotechnology, Nanomed. Nanotechnol. Biol. Med. 13 (3) (2017) 1137–1146.

[13] D. Jasinski, F. Haque, D.W. Binzel, P. Guo, Advancement of the emerging field of RNA nanotechnology, ACS Nano 11 (2) (2017) 1142–1164.

[14] X. Li, A.S. Bhullar, D.W. Binzel, P. Guo, The dynamic, motile and deformative properties of RNA nanoparticles facilitate the third milestone of drug development, Adv. Drug Deliv. Rev. 186 (2022), 114316.

[15] L. Rolband, D. Beasock, Y. Wang, Y.G. Shu, J.D. Dinman, T. Schlick, Y. Zhou, J. S. Kieft, S.J. Chen, G. Bussi, A. Oukhaled, X. Gao, P. Sulc, D. Binzel, A.S. Bhullar, C. Liang, P. Guo, K.A. Afonin, Biomotors, viral assembly, and RNA nanobiotechnology: current achievements and future directions, Comput. Struct. Biotechnol. J. 20 (2022) 6120–6137.

[16] B.E. Ferdows, D.N. Patel, W. Chen, X. Huang, N. Kong, W. Tao, RNA cancer nanomedicine: nanotechnology-mediated RNA therapy, Nanoscale 14 (12) (2022) 4448–4455.

[17] Y.X. Lin, Y. Wang, S. Blake, M. Yu, L. Mei, H. Wang, J. Shi, RNA nanotechnology-mediated cancer Immunotherapy, Theranostics 10 (1) (2020) 281–299.

[18] E.F. Khisamutdinov, H. Li, D.L. Jasinski, J. Chen, J. Fu, P. Guo, Enhancing Immunomodulation on Innate immunity by shape Transition among RNA Triangle, Square and Pentagon Nanovehicles, Nucleic Acids Res. 42 (15) (2014) 9996–10004.

[19] D.L. Jasinski, E.F. Khisamutdinov, Y.L. Lyubchenko, P. Guo, Physicochemically Tunable Polyfunctionalized RNA Square Architecture with Fluorogenic and Ribozymatic properties, ACS Nano 8 (8) (2014) 7620–7629.

[20] D.L. Jasinski, H. Li, P. Guo, The effect of size and shape of RNA nanoparticles on biodistribution, Mol. Ther. 26 (3) (2018) 784–792.

[21] X. Piao, H. Wang, D.W. Binzel, P. Guo, Assessment and comparison of thermal stability of Phosphorothioate-DNA, DNA, RNA, 2'-F RNA, and LNA in the Context of Phi29 pRNA 3WJ, RNA 24 (1) (2018) 67–76.

[22] X. Liu, D. Duan, Y. Wang, J. Liu, D. Duan, Advancements in 3WJ-based RNA nanotechnology and its application for cancer diagnosis and therapy, Front Biosci (Landmark Ed) 27 (2) (2022) 61.

[23] P. Guo, RNA nanotechnology: Engineering, assembly and applications in detection, gene delivery and therapy, J. Nanosci. Nanotechnol. 5 (12) (2005) 1964–1982.

[24] X. Piao, H. Yin, S. Guo, H. Wang, P. Guo, RNA nanotechnology to solubilize hydrophobic Antitumor drug for targeted delivery, Adv. Sci. 6 (22) (2019), 1900951.

[25] D. Shu, H. Li, Y. Shu, G. Xiong, W.E. Carson 3rd, F. Haque, R. Xu, P. Guo, Systemic delivery of anti-miRNA for suppression of Triple negative breast cancer utilizing RNA nanotechnology, ACS Nano 9 (10) (2015) 9731–9740.

[26] D. Binzel, Y. Shu, H. Li, M. Sun, Q. Zhang, D. Shu, B. Guo, P. Guo, Specific delivery of MiRNA for high efficient inhibition of Prostate cancer by RNA nanotechnology, Mol. Ther. 24 (2016) 1267–1277.

[27] D. Cui, C. Zhang, B. Liu, Y. Shu, T. Du, D. Shu, K. Wang, F. Dai, Y. Liu, C. Li, F. Pan, Y. Yang, J. Ni, H. Li, B. Brand-Saberi, P. Guo, Regression of Gastric cancer by systemic injection of RNA nanoparticles carrying both ligand and siRNA, Sci. Rep. 5 (2015) 10726–10739.

[28] Y. Xu, L. Pang, H. Wang, C. Xu, H. Shah, P. Guo, D. Shu, S.Y. Qian, Specific delivery of Delta-5-desaturase siRNA via RNA nanoparticles supplemented with

Dihomo-gamma-linolenic acid for colon cancer suppression, redox, Biol. 21 (2019) 101085–101093.

[29] D.W. Binzel, S. Guo, H. Yin, T.J. Lee, S. Liu, D. Shu, P. Guo, Rational design for controlled release of Dicer-substrate siRNA harbored in phi29 pRNA-based nanoparticles, Mol. Ther. Nucleic Acids 25 (2021) 524–535.

[30] M. Jang, H.D. Han, H.J. Ahn, A RNA nanotechnology platform for a simultaneous two-in-one siRNA delivery and its application in synergistic RNAi therapy, Sci. Rep. 6 (2016), 32363.

[31] L. Guo, D. Shi, M. Shang, X. Sun, D. Meng, X. Liu, X. Zhou, J. Li, Utilizing RNA nanotechnology to construct negatively charged and ultrasound-responsive nanodroplets for targeted delivery of siRNA, Drug Deliv. 29 (1) (2022) 316–327.

[32] A. Sharma, F. Haque, F. Pi, L.S. Shlyakhtenko, B.M. Evers, P. Guo, Controllable self-assembly of RNA Dendrimers, Nanomedicine 12 (3) (2016) 835–844.

[33] Z. Zheng, Z. Li, C. Xu, B. Guo, P. Guo, Folate-displaying Exosome mediated Cytosolic delivery of siRNA avoiding endosome trapping, J. Contr. Release 311–312 (2019) 43–49.

[34] S. Guo, M. Vieweger, K. Zhang, H. Yin, H. Wang, X. Li, S. Li, S. Hu, A. Sparreboom, B.M. Evers, Y. Dong, W. Chiu, P. Guo, Ultra-thermostable RNA nanoparticles for solubilizing and high-yield loading of paclitaxel for breast cancer therapy, Nat. Commun. 11 (1) (2020) 972.

[35] Y. Shu, H. Yin, M. Rajabi, H. Li, M. Vieweger, S. Guo, D. Shu, P. Guo, RNA-based Micelles: a novel platform for paclitaxel loading and delivery, J. Contr. Release 276 (2018) 17–29.

[36] H. Wang, S. Ellipilli, W.J. Lee, X. Li, M. Vieweger, Y.S. Ho, P. Guo, Multivalent Rubber-like RNA nanoparticles for targeted Co-delivery of paclitaxel and MiRNA to Silence the drug Efflux Transporter and liver cancer drug resistance, J. Contr. Release 330 (2020) 173–184.

[37] C. Ghimire, H. Wang, H. Li, M. Vieweger, C. Xu, P. Guo, RNA nanoparticles as Rubber for Compelling vessel Extravasation to enhance tumor targeting and for fast renal excretion to reduce toxicity, ACS Nano 14 (10) (2020) 13180–13191.

[38] C. Xu, F. Haque, D.L. Jasinski, D.W. Binzel, D. Shu, P. Guo, Favorable biodistribution, specific targeting and conditional endosomal Escape of RNA nanoparticles in cancer therapy, Cancer Lett. 414 (2018) 57–70.

[39] S.Y. Lee, C.Y. Yang, C.L. Peng, M.F. Wei, K.C. Chen, C.J. Yao, M.J. Shieh, A theranostic micelleplex co-delivering SN-38 and VEGF siRNA for colorectal cancer therapy, Biomaterials 86 (2016) 92–105.

[40] O. Takayuki, K. Kazushige, H. Keisuke, M. Koji, E. Shigenobu, K. Manabu, S. Kazuhito, N. Takeshi, T. Toshiaki, N. Hiroaki, SN-38 acts as a Radiosensitizer for colorectal cancer by inhibiting the Radiation-induced up-regulation of HIF-1α, Anticancer Res. 38 (6) (2018) 3323.

[41] V.A. Elliott, P. Rychahou, Y.Y. Zaytseva, B.M. Evers, Activation of c-Met and upregulation of CD44 expression are associated with the metastatic phenotype in the colorectal cancer liver metastasis model, PLoS One 9 (5) (2014), e97432.

[42] P. Rychahou, Y. Bae, D. Reichel, Y.Y. Zaytseva, E.Y. Lee, D. Napier, H.L. Weiss, N. Roller, H. Frohman, A.-T. Le, B. Mark Evers, Colorectal cancer lung metastasis treatment with polymer-drug nanoparticles, J. Contr. Release : official journal of the Controlled Release Society 275 (2018) 85–91.

[43] D. Shu, Y. Shu, F. Haque, S. Abdelmawla, P. Guo, Thermodynamically stable RNA three-way junction for constructing multifunctional nanoparticles for delivery of therapeutics, Nat. Nanotechnol. 6 (10) (2011) 658–667.

[44] Y. Zhang, M. Leonard, Y. Shu, Y. Yang, D. Shu, P. Guo, X. Zhang, Overcoming Tamoxifen resistance of human breast cancer by targeted gene Silencing using multifunctional pRNA nanoparticles, ACS Nano 11 (1) (2017) 335–346.

[45] F. Pi, D.W. Binzel, T.J. Lee, Z. Li, M. Sun, P. Rychahou, H. Li, F. Haque, S. Wang, C.M. Croce, B. Guo, B.M. Evers, P. Guo, Nanoparticle orientation to control RNA loading and ligand display on extracellular vesicles for cancer regression, Nat. Nanotechnol. 13 (1) (2018) 82–89.

[46] Y. Hao, J.S. Kieft, Diverse self-association properties within a family of phage packaging RNAs, RNA 20 (11) (2014) 1759–1774.

[47] C. Zhang, M. Trottier, C. Chen, P. Guo, Chemical modification patterns of active and inactive as well as procapsid-bound and unbound DNA-packaging RNAof bacterial virus Phi29, Virology 281 (2) (2001) 281–293.

[48] S. Hoeprich, Q. Zhou, S. Guo, D. Shu, G. Qi, Y. Wang, P. Guo, Bacterial virus phi29 pRNA as a hammerhead ribozyme escort to destroy hepatitis B virus, Gene Ther. 10 (15) (2003) 1258–1267.

[49] A. Zou, S. Lee, J. Li, R. Zhou, Retained stability of the RNA structure in DNA packaging motor with a single Mg(2+) Ion bound at the double Mg-Clamp structure, J. Phys. Chem. B 124 (5) (2020) 701–707.

[50] A.C. Hill, J.S. Schroeder, Thermodynamic stabilities of three-way junction nanomotifs in prohead RNA, RNA 23 (4) (2017) 521–529.

[51] S. Guo, C. Xu, H. Yin, J. Hill, F. Pi, P. Guo, Tuning the size, shape and structure of RNA nanoparticles for favorable cancer targeting and immunostimulation, Wiley Interdiscip Rev Nanomed Nanobiotechnol 12 (1) (2020), e1582.

[52] S. Guo, H. Li, M. Ma, J. Fu, Y. Dong, P. Guo, Size, shape, and sequence-dependent immunogenicity of RNA nanoparticles, Mol. Ther. Nucleic Acids 9 (2017) 399–408.

[53] D.W. Binzel, E. Khisamutdinov, M. Vieweger, J. Ortega, J. Li, P. Guo, Mechanism of three-component collision to produce ultrastable pRNA three-way junction of Phi29 DNA-packaging motor by kinetic assessment, RNA (New York, N.Y.) 22 (11) (2016) 1710–1718.

[54] D. Shu, E.F. Khisamutdinov, L. Zhang, P. Guo, Programmable folding of Fusion RNA in vivo and in vitro Driven by pRNA 3WJ motif of Phi29 DNA packaging motor, Nucleic Acids Res. 42 (2) (2014) e10.

[55] P. Guo, Y. Shu, D. Binzel, M. Cinier, Synthesis, conjugation, and labeling of multifunctional pRNA nanoparticles for specific delivery of siRNA, drugs, and other therapeutics to target cells, Methods Mol. Biol. 928 (2012) 197–219.

[56] Y. Shu, M. Cinier, D. Shu, P. Guo, Assembly of multifunctional phi29 pRNA nanoparticles for specific delivery of siRNA and other therapeutics to targeted cells, Methods 54 (2) (2011) 204–214.

[57] B. Huang, W.D. Abraham, Y. Zheng, S.C. Bustamante Lopez, S.S. Luo, D.J. Irvine, Active targeting of chemotherapy to disseminated tumors using nanoparticle-carrying T cells, Sci. Transl. Med. 7 (291) (2015) 291ra94.

[58] I.S. Alferiev, R. Iyer, J.L. Croucher, R.F. Adamo, K. Zhang, J.L. Mangino, V. Kolla, I. Fishbein, G.M. Brodeur, R.J. Levy, M. Chorny, Nanoparticle-mediated delivery of a rapidly activatable prodrug of SN-38 for neuroblastoma therapy, Biomaterials 51 (2015) 22–29.

[59] A.D. Keefe, S. Pai, A. Ellington, Aptamers as therapeutics, Nat. Rev. Drug Discov. 9 (7) (2010) 537–550.

[60] O. Gires, M. Pan, H. Schinke, M. Canis, P.A. Baeuerle, Expression and function of epithelial cell adhesion molecule EpCAM: where are we after 40 years? Cancer Metastasis Rev. 39 (3) (2020) 969–987.

[61] S. Shigdar, J. Lin, Y. Yu, M. Pastuovic, M. Wei, W. Duan, RNA aptamer against a cancer stem cell marker epithelial cell adhesion molecule, Cancer Sci. 102 (5) (2011) 991–998.

[62] S. Hu, E. Lee, C. Wang, J. Wang, Z. Zhou, Y. Li, X. Li, J. Tang, D.H. Lee, X. Liu, Y. Shen, Amphiphilic drugs as surfactants to fabricate excipient-free stable nanodispersions of hydrophobic drugs for cancer chemotherapy, J. Contr. Release 220 (Pt A) (2015) 175–179.

[63] M.S. Surapaneni, S.K. Das, N.G. Das, Designing Paclitaxel drug delivery systems aimed at improved patient outcomes: current status and challenges, ISRN Pharmacol 2012 (2012), 623139.

[64] D.I. Jang, A.H. Lee, H.Y. Shin, H.R. Song, J.H. Park, T.B. Kang, S.R. Lee, S. H. Yang, The Role of tumor necrosis factor Alpha (TNF-alpha) in Autoimmune disease and current TNF-alpha Inhibitors in therapeutics, Int. J. Mol. Sci. 22 (5) (2021).

[65] T. Tanaka, M. Narazaki, T. Kishimoto, IL-6 in inflammation, immunity, and disease, Cold Spring Harb Perspect Biol 6 (10) (2014) a016295.

[66] C. Caldari-Torres, J. Beck, Effects of co-incubation of LPS-stimulated RAW 264.7 macrophages on leptin production by 3T3-L1 adipocytes: a method for co-incubating distinct adipose tissue cell lines, Bull. Natl. Res. Cent. 46 (1) (2022) 57.

[67] R. Bayat Mokhtari, T.S. Homayouni, N. Baluch, E. Morgatskaya, S. Kumar, B. Das, H. Yeger, Combination therapy in combating cancer, Oncotarget 8 (23) (2017) 38022–38043.

[68] S. Gurunathan, M.H. Kang, M. Qasim, J.H. Kim, Nanoparticle-mediated combination therapy: two-in-one approach for cancer, Int. J. Mol. Sci. 19 (10) (2018).

[69] P. Guo, C. Zhang, C. Chen, K. Garver, M. Trottier, Inter-RNA interaction of phage Phi29 pRNA to form a Hexameric complex for viral DNA Transportation, Mol. Cell 2 (1) (1998) 149–155.

[70] P. Rychahou, F. Haque, Y. Shu, Y. Zaytseva, H.L. Weiss, E.Y. Lee, W. Mustain, J. Valentino, P. Guo, B.M. Evers, Delivery of RNA nanoparticles into colorectal cancer metastases following systemic administration, ACS Nano 9 (2) (2015) 1108–1116.

[71] F. Pi, H. Zhang, H. Li, V. Thiviyanathan, D.G. Gorenstein, A.K. Sood, P. Guo, RNA nanoparticles harboring annexin A2 aptamer can target ovarian cancer for tumor-specific doxorubicin delivery, Nanomedicine 13 (3) (2017) 1183–1193.

[72] T.J. Lee, J.Y. Yoo, D. Shu, H. Li, J. Zhang, J.G. Yu, A.C. Jaime-Ramirez, M. Acunzo, G. Romano, R. Cui, H.L. Sun, Z. Luo, M. Old, B. Kaur, P. Guo, C. M. Croce, RNA nanoparticle-based targeted therapy for Glioblastoma through inhibition of Oncogenic miR-21, Mol. Ther. 25 (7) (2017) 1544–1555.

[73] Y. Shu, D. Shu, Z. Diao, G. Shen, P. Guo, Fabrication of Polyvalent therapeutic RNA nanoparticles for specific delivery of siRNA, ribozyme and drugs to targeted cells for cancer therapy, IEEE NIH Life Sci. Syst. Appl. Workshop (2009) 9–12, 2009.

[74] M.M. Fay, S.M. Lyons, P. Ivanov, RNA G-Quadruplexes in Biology: Principles and molecular mechanisms, J. Mol. Biol. 429 (14) (2017) 2127–2147.

[75] W. Zhang, S.J. Chen, RNA hairpin-folding kinetics, Proc Natl Acad Sci U S A 99 (4) (2002) 1931–1936.

[76] H. Ma, D.J. Proctor, E. Kierzek, R. Kierzek, P.C. Bevilacqua, M. Gruebele, Exploring the energy landscape of a small RNA hairpin, J. Am. Chem. Soc. 128 (5) (2006) 1523–1530.

[77] H. Qiu, K. Kaluarachchi, Z. Du, D.W. Hoffman, D.P. Giedroc, Thermodynamics of folding of the RNA pseudoknot of the T4 gene 32 autoregulatory messenger RNA, Biochemistry 35 (13) (1996) 4176–4186.

[78] K. Jin, Y.C. Liao, T.C. Cheng, X. Li, W.J. Lee, F. Pi, D. Jasinski, L.C. Chen, M. A. Phelps, Y.S. Ho, P. Guo, In Vitro and In Vivo Evaluation of the Pathology and Safety Aspects of Three- and Four-Way Junction RNA Nanoparticles, Mol Pharmaceut (2023 In Press).

[79] H. Yin, G. Xiong, S. Guo, C. Xu, R. Xu, P. Guo, D. Shu, Delivery of anti-miRNA for Triple-negative breast cancer therapy using RNA nanoparticles targeting stem cell marker CD133, Mol. Ther. 27 (7) (2019) 1252–1261.

[80] B.W. Neun, A.N. Ilinskaya, M.A. Dobrovolskaia, Updated method for in vitro analysis of nanoparticle Hemolytic properties, Methods Mol. Biol. 1682 (2018) 91–102.

[81] J. Rodriguez, E. Cedrone, B. Neun, M. Dobrovolskaia, NCL Method ITA-2.2 (2020).

[82] B.W. Neun, A.N. Ilinskaya, M.A. Dobrovolskaia, Analysis of complement activation by nanoparticles, Methods Mol. Biol. 1682 (2018) 149–160.

[83] E. Cedrone, T. Potter, B. Neun, M. Dobrovolskaia, NCL Method ITA- 12 (2020).

[84] T.M. Potter, B.W. Neun, J.C. Rodriguez, A.N. Ilinskaya, M.A. Dobrovolskaia, Analysis of pro-inflammatory cytokine and type II interferon induction by nanoparticles, Methods Mol. Biol. 1682 (2018) 173–187.

[85] B. Neun, J. Rodriguez, T. Potter, A. Ilinskaya, M. Dobrovolskaia, NCL Method ITA- 25 (2020).

[86] E. Cedrone, T. Potter, B. Neun, A. Tyler, M. Dobrovolskaia, NCL Method ITA- 27 (2021).

[87] C. Geary, A. Chworos, E. Verzemnieks, N.R. Voss, L. Jaeger, Composing RNA nanostructures from a Syntax of RNA structural Modules, Nano Lett. 17 (11) (2017) 7095–7101.

[88] W.W. Grabow, P. Zakrevsky, K.A. Afonin, A. Chworos, B.A. Shapiro, L. Jaeger, Self-assembling RNA Nanorings based on RNAI/II Inverse Kissing complexes, Nano Lett. 11 (2) (2011) 878–887.

[89] K.A. Afonin, D.J. Cieply, N.B. Leontis, Specific RNA self-assembly with minimal Paranemic motifs, J. Am. Chem. Soc. 130 (1) (2008) 93–102.

[90] S.A. Woodson, RNA folding and ribosome assembly, Curr. Opin. Chem. Biol. 12 (6) (2008) 667–673.

[91] D.R. Duckett, A.I. Murchie, D.M. Lilley, The Global folding of four-way helical junctions in RNA, including that in U1 snRNA, Cell 83 (6) (1995) 1027–1036.

[92] K.A. Afonin, M. Viard, A.Y. Koyfman, A.N. Martins, W.K. Kasprzak, M. Panigaj, R. Desai, A. Santhanam, W.W. Grabow, L. Jaeger, E. Heldman, J. Reiser, W. Chiu, E.O. Freed, B.A. Shapiro, Multifunctional RNA nanoparticles, Nano Lett. 14 (10) (2014) 5662–5671.

[93] M. Paliy, R. Melnik, B.A. Shapiro, Molecular dynamics study of the RNA ring nanostructure: a Phenomenon of self-stabilization, Phys. Biol. 6 (4) (2009) 46003–46016.

[94] E. Westhof, B. Masquida, L. Jaeger, RNA Tectonics: towards RNA design, Fold Des 1 (4) (1996) R78–R88.

[95] L. Jaeger, N.B. Leontis, Tecto-RNA: one-dimensional self-assembly through Tertiary interactions, Angew. Chem., Int. Ed. Engl. 39 (14) (2000) 2521–2524.

[96] L. Jaeger, E. Westhof, N.B. Leontis, TectoRNA: Modular assembly units for the construction of RNA Nano-objects, Nucleic Acids Res. 29 (2) (2001) 455–463.

[97] E. Bindewald, C. Grunewald, B. Boyle, M. O'Connor, B.A. Shapiro, Computational Strategies for the Automated design of RNA Nanoscale structures from Building Blocks using NanoTiler, J. Mol. Graph. Model. 27 (3) (2008) 299–308.

[98] I. Severcan, C. Geary, E. Verzemnieks, A. Chworos, L. Jaeger, Square-shaped RNA particles from different RNA folds, Nano Lett. 9 (3) (2009) 1270–1277.

[99] D. Jedrzejczyk, A. Chworos, Self-Assembling RNA nanoparticle for gene expression regulation in a model system, ACS Synth. Biol. 8 (3) (2019) 491–497.

[100] C. Xu, H. Li, K. Zhang, D.W. Binzel, H. Yin, W. Chiu, P. Guo, Photo-controlled release of paclitaxel and model drugs from RNA Pyramids, Nano Res. 12 (2019) 41–48.

[101] Y. Shu, F. Haque, D. Shu, W. Li, Z. Zhu, M. Kotb, Y. Lyubchenko, P. Guo, Fabrication of 14 different RNA nanoparticles for specific tumor targeting without accumulation in normal organs, RNA (New York, N.Y.) 19 (6) (2013) 767–777.

[102] H. Yin, H. Wang, Z. Li, D. Shu, P. Guo, RNA Micelles for the systemic delivery of anti-miRNA for cancer targeting and inhibition without ligand, ACS Nano 13 (1) (2019) 706–717.

[103] H. Li, K. Zhang, F. Pi, S. Guo, L. Shlyakhtenko, W. Chiu, D. Shu, P. Guo, Controllable self-assembly of RNA Tetrahedrons with precise shape and size for cancer targeting, Adv. Mater. 28 (34) (2016) 7501–7507.

[104] P.X. Guo, B. Moss, Interaction and Mutual stabilization of the two subunits of Vaccinia virus mRNA capping enzyme Coexpressed in Escherichia Coli, Proc. Natl. Acad. Sci. U.S.A. 87 (11) (1990) 4023–4027.

[105] S.M. Hoy, Patisiran: First Global approval, Drugs 78 (15) (2018) 1625–1631.

[106] L.J. Scott, S.J. Keam, Lumasiran: First approval, Drugs 81 (2) (2021) 277–282.

[107] L.J. Scott, Givosiran: First approval, Drugs 80 (3) (2020) 335–339.

[108] Y. Shu, D. Shu, F. Haque, P.X. Guo, Fabrication of pRNA nanoparticles to deliver therapeutic RNAs and bioactive compounds into tumor cells, Nat. Protoc. 8 (9) (2013) 1635–1659.

[109] K.A. Afonin, D. Schultz, L. Jaeger, E. Gwinn, B.A. Shapiro, Silver nanoclusters for RNA nanotechnology: steps towards visualization and tracking of RNA nanoparticle assemblies, Methods Mol. Biol. 1297 (2015) 59–66.

[110] H. Li, T. Lee, T. Dziubla, F. Pi, S. Guo, J. Xu, C. Li, F. Haque, X.-J. Liang, P. Guo, RNA as a stable polymer to build controllable and defined nanostructures for material and biomedical applications, Nano Today 10 (5) (2015) 631–655.

[111] K.A. Afonin, B. Lindsay, B.A. Shapiro, Engineered RNA Nanodesigns for applications in RNA nanotechnology, DNA RNA Nanotechnol. 1 (1) (2015) 1–15.

[112] G.C. Shukla, F. Haque, Y. Tor, L.M. Wilhelmsson, J.J. Toulme, H. Isambert, P. Guo, J.J. Rossi, S.A. Tenenbaum, B.A. Shapiro, A boost for the emerging field of RNA nanotechnology, ACS Nano 5 (5) (2011) 3405–3418.

[113] M.M. Tolba, A. Jabbar, S. Afzal, M. Mahmoud, F. Zulfiqar, I. El-Soudany, S. Samir, A.S. Wadan, T.E. Ellakwa, D.E. Ellakwa, A promising RNA nanotechnology in clinical therapeutics: a future perspective narrative review, Future Sci OA 9 (8) (2023) FSO883.

[114] T. Lv, Y. Meng, Y. Liu, Y. Han, H. Xin, X. Peng, J. Huang, RNA nanotechnology: a new chapter in targeted therapy, Colloids Surf. B Biointerfaces 230 (2023), 113533.